Pertanika J. Sci. & Technol. 33 (1): 121 - 147 (2025)

PERTANIKA JOURNALS

SCIENCE & TECHNOLOGY

Journal homepage: http://www.pertanika.upm.edu.my/

Review Article

A Focused Review on Upper and Lower Limb Joint Torque Estimation via Neural Networks

Chamalka Kenneth Perera[1], Alpha Agape Gopalai[1]*, Darwin Gouwanda[1] and Siti Anom Ahmad[2]

[1]School of Engineering, Monash University, 47500 Subang Jaya, Bandar Sunway, Selangor, Malaysia
[2]Department of Electrical and Electronic Engineering, Faculty of Engineering, Universiti Putra Malaysia, 43400 UPM, Serdang, Selangor, Malaysia

ABSTRACT

Joint torque estimation is an essential aspect of the control architecture in assistive devices for rehabilitation and aiding movement impairments. Healthy adult torque trajectories serve as a baseline for controllers to determine the level of assistance required by patients, evaluate impaired motion, understand biomechanics, and design treatment plans. Currently, methods of torque estimation include inverse dynamics using gold standard motion capture systems, generic mathematical models based on joint torque-angle relationships, neuromusculoskeletal modelling using surface electromyography, and neural networks. As such, this review provides a focused overview of the recent and existing neural networks tailored for upper and lower limb joint torque estimation. Dataset preparation, data preprocessing, and evaluation metrics are presented along with a detailed description of the developed networks, which are classified by model architecture. It includes artificial neural networks (ANNs), convolution neural networks (CNNs), long short-term memory (LSTM) networks, and hybrid and alternate architectures such as wavelet or explainable convolution (XCM). The performance, benefits, and limitations of the models are discussed, highlighting CNNs and LSTMs as the current optimal models for time series prediction of joint torque. This is due to their ability to capture spatial and temporal dependencies in the data. Additionally, joint kinematics such as angles, angular velocities, and accelerations are considered optimal input parameters due to their ease of measurement using wearable sensors and integration with wearable assistive technology.

Keywords: ANN, artificial intelligence, CNN, control architecture, joint moments, LSTM, torque estimation

ARTICLE INFO

Article history:
Received: 06 February 2024
Accepted: 19 August 2024
Published: 27 January 2025

DOI: https://doi.org/10.47836/pjst.33.1.06

E-mail addresses:
chamalka.perera@monash.edu (Chamalka Kenneth Perera)
alpha.agape@monash.edu (Alpha Agape Gopalai)
darwin.gouwand@monash.edu (Darwin Gouwanda)
sanom@upm.edu.my (Siti Anom Ahmad)
* Corresponding author

ISSN: 0128-7680
e-ISSN: 2231-8526

INTRODUCTION

Addressing the challenges of ageing and movement impairment is necessary for individuals to maintain a good quality of life (Kruk et al., 2022). To support this, wearable assistive devices (such as exoskeletons or soft exosuits) are gaining significance for assisting impaired motion during rehabilitation or daily tasks (Liu et al., 2019; Schmidt et al., 2017). A key aspect of these devices is their controllers, which utilise joint torque estimation models to obtain a benchmark that sets and tracks the level of assistance for a patient (Moreira et al., 2021). Reference torque trajectories ensure adequate assistance is supplied to the user to complete a motion and are also important in understanding biomechanics and impaired movement and when evaluating the effectiveness of treatments (Perera et al., 2023). Hence, the progression of torque estimation methods would further assistive devices' design and control architectures. Yet, deriving torque trajectories can be complex, requiring extensive processing techniques with calculations using mathematical or human biomechanical models (Siu et al., 2021; Wang & Buchanan, 2002).

Currently, four main approaches exist for torque estimation: (1) inverse dynamics (ID), (2) mathematical modelling, (3) neuromusculoskeletal (NMS) modelling and (4) neural networks (Dinovitzer et al., 2023; Liu et al., 2019; Zhang, Soselia et al., 2023). ID involves tracking motion kinematics and external ground reaction forces (GRFs) using optical motion capture (Mocap) systems and force plates or inertial measurement units (IMUs). The Mocap data combines approximations for body segment inertia or point mass utilising kinematic link segment models. Newton-Euler or Lagrange equations of motion are used to derive joint torques with tools such as OpenSim (Delp et al., 2007; Seth et al., 2018) or Visual 3D (C-Motion Inc.). Despite ID being the gold standard for calculating joint torques, they require expensive and bulky laboratory setups, which are not ideal for integrating wearable devices (Dinovitzer et al., 2023; Siu et al., 2021). Further, mathematical models based on a linear approximation of the joint torque-angle relationship can be applied for selected movements, as proposed in the exoskeleton and exosuit by Liu et al. (2019) and Schmidt et al. (2017), respectively. While these models are easily integrated into controllers, they are generic and do not account for variations in subject characteristics such as age, anthropometry, or movement strategies (Moreira et al., 2021; Perera et al., 2023). Alternatively, NMS modelling (Figure 1) utilises surface electromyography (SEMG) signals, which measure the electric current field caused by the depolarisation of muscle fibres due to an action potential (Farina & Enoka, 2023). It calculates muscle activation via neural excitation with reference to a Hill-type muscle model (activation dynamics). Through contraction dynamics, muscle activation is used to determine muscle force (accounting for force-length/velocity relationships) and then, in conjunction with joint moment-arms, produces torque (Wang & Buchanan, 2002). Modelling tools like OpenSim with toolboxes like CEINMS (Pizzolato et al., 2015) are commonly employed for this

analysis. However, NMS modelling requires tedious calibration and processing techniques for each subject individually, while SEMG signals are inherently noisy and affected by muscle crosstalk, sweat, and displacement during motion. Hence, they are difficult to use in wearable devices for prolonged periods (Farina & Enoka, 2023; Moreira et al., 2021; Zhang, Soselia et al., 2023).

Thus, neural networks have gained prominence in torque estimation to overcome the limitations of the previous methods (Figure 1). These networks do not require a human body model; they map directly from sensor input to output torque and are good at predicting non-linear behaviour while capturing spatial and temporal information (Li et al., 2020). The benefit is that neural networks can estimate each user's dynamically varying torque

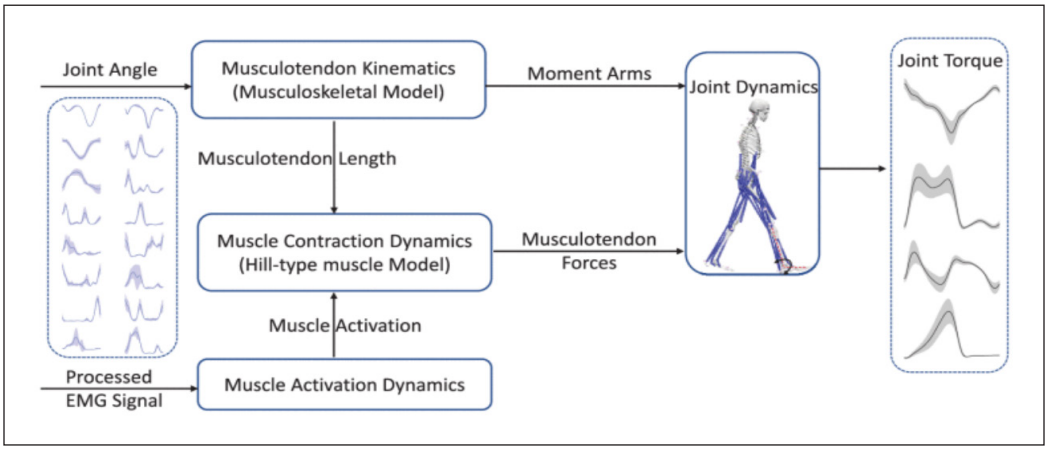

(a)

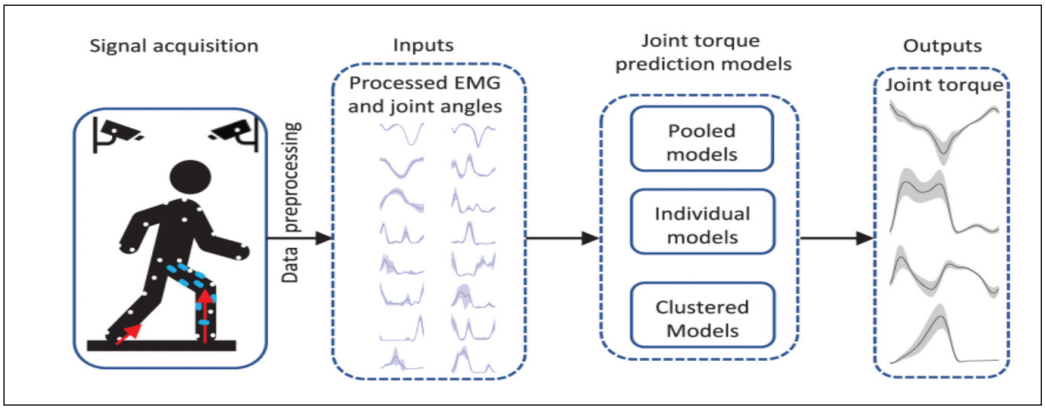

(b)

Figure 1. (a) An overview of neuromusculoskeletal (NMS) modelling for estimating joint torques using electromyography (EMG) signals, a Hill-type muscle model, and OpenSim. (b) Outline of a neural network architecture for joint torque estimation consisting of pooled, individual, and clustered network models. Reprinted and modified with permission from (Zhang et al., 2023) and published under the Creative Commons Attribution License (CC BY 4.0)

requirements while providing personalised trajectories based on subject characteristics such as age or anthropometry for more effective and natural assistance (Moreira et al., 2021). Deep learning models also eliminate the need for repetitive subject data collection and calibration or processing once trained (Mundt et al., 2021; Zhang, Soselia et al., 2022). However, the limitation is the black-box nature of these models, which masks the reasoning behind their prediction, and the relationships between input data and torque cannot be easily investigated. Additionally, the effectiveness of the network is highly dependent on the quality, quantity, and variety of training data which is necessary to ensure model generalisability (Siu et al., 2021; Wang & Buchanan, 2002; Zhang, Soselia et al., 2022).

This study aims to review existing neural network approaches for estimating upper and lower limb joint torques. The literature referenced in this study comprises different neural network architectures, input parameters, preprocessing techniques, evaluation metrics, and joint motions. The following sections present these findings and recommendations on the optimal model architectures and input parameters for joint torque estimation. Future perspectives targeted towards wearable assistive technology are also discussed.

METHODS

PubMed and Scopus databases were searched for scientific articles involving neural networks that estimate upper and lower limb joint torques based on their title, abstract, keywords, and relevance (Figure 2). The search keywords were joint torques, joint moments, neural networks, deep learning, torque estimation, and torque prediction. The exclusion

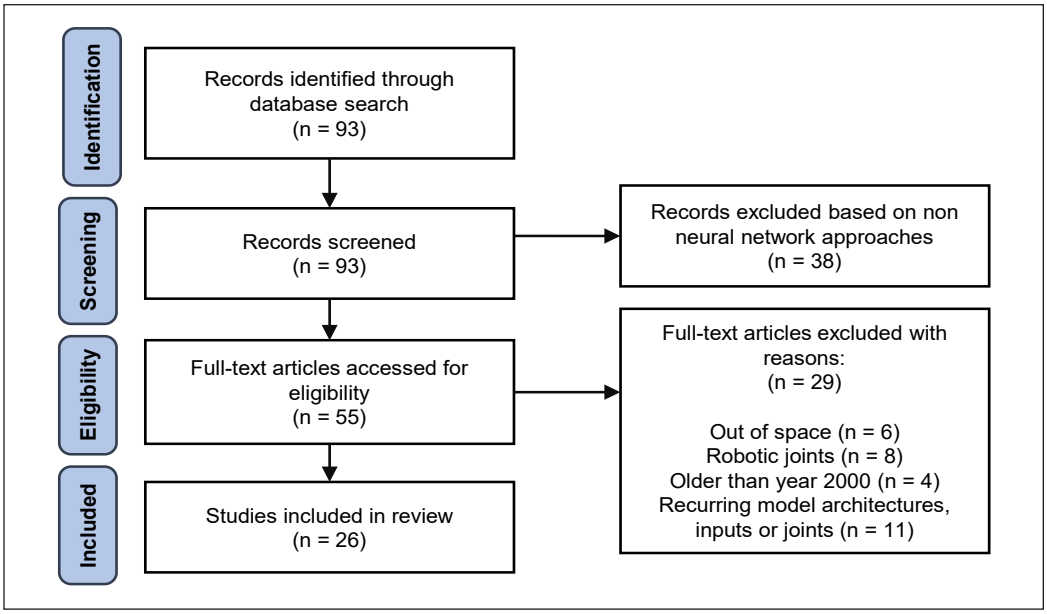

Figure 2. Number of articles identified for review on upper and lower limb joint torque estimation via neural networks

criteria were publications containing robotic joint torques, non-neural network approaches, articles older than the year 2000 and similar articles with repeating model architectures, input parameters and targeted lower or upper limb joints.

MAJOR FINDINGS

Numerous neural networks have been proposed for torque estimation utilising a range of input parameters and are categorised based on their model type, as presented in Table 1. Artificial neural networks (ANNs) consist of fully connected layers, which form the basis for more complex architectures. In these dense or multi-layer perceptron networks, each neuron per layer is connected to every neuron in the next layer, with adjustable weights and multiple hidden layers (Chandrapal et al., 2011). Similarly, time delay neural networks (TDNNs) build on ANNs by introducing delays or convolutions to extract temporal features in sequential data (Peng et al., 2015).

Convolution neural networks (CNNs) process images or grid-structured data using convolution and pooling operators coupled with non-linear activation functions to recognise spatial information effectively (Taye, 2023). Alternatively, long short-term memory (LSTM) neural networks are a recurrent neural network (RNN) type that can identify temporal features using memory cells and a gated structure comprising forget, input, and output gates to update cell and hidden states. LSTMs are particularly effective in capturing long-term dependencies and analysing time series data (Cho et al., 2014; Zhang, Soselia et al., 2022). Additionally, hybrid networks use a sequential combination of deep learning with mathematical or NMS models. Instead of directly estimating torque, the hybrid networks predict alternate parameters like GRFs or muscle activations, which are then used as inputs into mathematical (for example, ID and gravity compensation equations) or computational NMS models to derive torque (Lam & Vujaklija, 2021; Wang & Buchanan, 2002).

Dataset Preparation and Preprocessing

Neural networks for joint torque estimation use a variety of data types and sources for model training and testing. Kinematic and kinetic data are obtained either through optical Mocap systems and force plates or through wearable sensors like IMUs, encoders, or electrogoniometers (Altai et al., 2023; Dinovitzer et al., 2023; Liu et al., 2009). SEMG data provides muscle activity linked to joint torque, typically collected from the muscles involved in a joint motion (Chandrapal et al., 2011). Subject anthropometry like age, weight, or height are also considered when creating personalised torque estimation models (Moreira et al., 2021). From this, diverse and large-scale datasets should be considered for training to account for variability in human movement, subject characteristics, and generalizability of the models to a subject population.

Table 1
Overview of the existing neural networks for upper and lower limb joint torque estimation

Model Type	Reference	Motion	Output Joint Torques	Input Parameters	Sample Size
Artificial neural networks	McCabe et al., 2023	Stair ascent	Hip flexion, extension, adduction, and abduction.	GRFs with shank and thigh IMU data.	17 healthy adults.
	Mundt et al., 2020	Gait	Hip, knee, and ankle in sagittal, coronal, and transverse planes.	Hip, knee, and ankle joint accelerations and angular velocities.	30 healthy adults.
	Molinaro et al., 2020	Gait and ramp ascent/ descent.	Hip flexion and extension.	Hip joint angle and thigh IMU.	5 healthy adults.
	Lim et al., 2019	Gait at varying speeds.	Hip, knee, and ankle in sagittal plane.	COM kinematics.	7 healthy adults.
	Chandrapal et al., 2011	Isometric and isokinetic knee movements.	Knee flexion and extension.	SEMG from 5 knee extensor and flexor muscles.	Single subject over 10 days.
	Liu et al., 2009	Squat and counter-movement jump.	Hip, knee, and ankle in sagittal plane.	GRFs.	10 healthy adults.
Time delay neural networks	Su et al., 2020	Ankle movement using a Biodex rehabilitation machine.	Ankle inversion and eversion.	SEMG from 5 lower body muscles with ankle angular velocity.	5 healthy adults and 3 rehabilitation patients.
	Peng et al., 2015	Elbow movement with arms vertical and parallel to the ground.	Elbow flexion and extension.	SEMG of two upper body muscles with joint angles and angular velocity.	4 healthy adults.
Convolution neural networks	Ozates et al., 2023	Gait	Hip, knee, and ankle in sagittal plane, with hip adduction and abduction.	Trunk, pelvis, hip, knee, and ankle joint angles in sagittal, coronal, and transverse planes.	132 healthy adults and 622 patients with cerebral palsy.
	Zhang, Fragnito et al., 2022	Gait at varying walking speeds.	Ankle plantar flexion.	Brightness mode ultrasound images of skeletal muscles.	8 healthy adults.
	Yu et al., 2022	Isometric wrist movements.	Wrist flexion, extension, pronation, and supination.	SEMG arrays for muscles around the forearm.	8 healthy adults.

Table 1 *(continue)*

Model Type	Reference	Motion	Output Joint Torques	Input Parameters	Sample Size
	Moreira et al., 2021	Gait at varying walking speeds.	Ankle dorsiflexion and plantar flexion.	Ankle joint angles, angular velocity, and angular acceleration with walking speed, height, mass, foot length, sex, and age.	13 healthy adults.
	Hajian et al., 2021	Isotonic, isokinetic, and dynamic elbow movements from a Biodex rehabilitation machine.	Elbow flexion and extension.	SEMG from 4 upper body muscles with position and velocity.	5 healthy adults.
Long short-term memory neural networks	Zhang et al., 2023	Fast, normal, and slow walking with sit-to-stand, stand-to-sit, squat, jump, land, jump-up-to-stair, and jump-down-from stair.	Hip, knee, and ankle in sagittal plane, with hip adduction and abduction.	SEMG from 13 lower body muscles with hip, knee, and ankle joint angles.	8 healthy adults.
	Wang et al., 2023	Gait	Hip, knee, and ankle in sagittal plane.	SEMG from 5 lower body muscles with hip, knee, and ankle joint angles.	4 healthy adults.
	Truong et al., 2023	Squat, sit-to-stand, and object pick-up.	Knee and ankle in sagittal plane.	SEMG from 14 lower body muscles.	6 healthy adults.
	Zhang, Soselia et al., 2022	Fast, normal, and slow walking with sit-to-stand, stand-to-sit, squat, jump, land, jump-up-to-stair, and jump-down-from stair.	Hip, knee, and ankle in sagittal plane, with hip adduction and abduction.	SEMG from 13 lower body muscles with hip, knee, and ankle joint angles.	8 healthy adults.
	Siu et al., 2021	Standing, walking, running, and sprinting.	Ankle dorsiflexion and plantar flexion.	SEMG from 4 lower body muscles.	4 healthy adults.
Hybrid neural networks	Dinovitzer et al., 2023	Gait with starting, stopping, sudden speed changes and asymmetrical motion.	Hip, knee, and ankle in sagittal plane.	Joint kinematics with angles, velocity, accelerations, and segment positions.	11 healthy adults.

Table 1 *(continue)*

Model Type	Reference	Motion	Output Joint Torques	Input Parameters	Sample Size
	Schulte et al., 2022	Gait, stair ascent/ descent, ramp ascent/ descent, sit-to-stand, and non-weight-bearing activities.	Knee flexion and extension.	SEMG from 4 lower body muscles with knee joint angle and IMU data from 8 locations.	10 healthy adults.
	Lam & Vujaklija, 2021	Gait	Hip, knee, and ankle in sagittal planes.	SEMG from 8 lower body muscles with linear and angular kinematics.	5 healthy adults.
	Wang & Buchanan, 2002	Isometric elbow movement in the sagittal plane.	Elbow flexion and extension.	SEMG from 10 upper body muscles.	1 healthy adult.
InceptionTimePlus, XCM, XCMplus, RNNplus, and Time-series transformer.	Altai et al., 2023	Gait, stair ascent/ descent and ramp ascent/descent.	Hip, knee, and ankle in sagittal planes.	IMU data from trunk, thigh, shank, and foot.	22 healthy adults.
Non-linear autoregressive with exogenous inputs (NARX)	Li et al., 2020	Isometric elbow movement in the sagittal plane.	Elbow flexion and extension.	SEMG from 2 upper body muscles.	8 healthy adults.
Autoencoder with a back propagation neural network	Huang et al., 2020	Push and pull motion.	Shoulder and elbow flexion and extension.	SEMG from 6 upper body muscles with shoulder and elbow joint angles.	3 healthy adults.
Wavelet neural network	Ardestani et al., 2014	Gait	Hip, knee, and ankle in sagittal planes with hip adduction, abduction, rotation, and subtalar eversion.	SEMG from 14 lower body muscles with GRFs.	4 patients with knee prostheses.

Preprocessing of these input parameters is a vital step before model training. SEMG, for instance, is filtered to remove noise and rectify it, and low pass is filtered to create an envelope. It can be normalised using the maximum voluntary contraction (MVC). Features include the mean absolute value, root mean square (RMS), zero crossings, slope sign change, simple square integral, waveform length, myopulse percentage rate, and the mean or median frequencies (Chandrapal et al., 2011; Truong et al., 2023; Wang et al., 2023). SEMG can also be interpreted as a collection of RMS windows for real-time applications (Su et al., 2020) or a collection of 2D images/arrays at every sampling instant (Yu et al., 2022). Zhang, Fragnito et al. (2022) extended this by performing a continuous wavelet transform and organising SEMG into matrices with scale components of frequency-domain information for the time sequence of the signal. It was then compared against the brightness mode of ultrasound images from skeletal muscles for specific regions of interest.

Moreover, Mocap data, GRFs, IMU readings, and joint kinematics are also subject to appropriate filtering techniques. Lowpass and bandpass filters are used to remove noise and motion artifacts and for smoothing where filter cut-off frequencies can be selected by performing a Fast Fourier Transform and observing the signal bandwidth (Crenna et al., 2021; Winter, 2009). GRFs provide vertical, anteroposterior, and mediolateral force components along with the centre of pressure (COP) or zero-moment point (ZMP) (Dinovitzer et al., 2023). From IMUs, body segment accelerations, angular velocities, positions, and sensor orientations are collected, while joint angles can also be derived (Altai et al., 2023; Dinovitzer et al., 2023; Molinaro et al., 2020; Mundt et al., 2020). Additionally, centre of mass (COM) kinematics are also considered as they are a dynamic determinant for segment kinetics during gait. Features such as COM apex (maximum point in sagittal plane), position, and velocity were utilised (Lim et al., 2019).

All data types of the input parameters are formatted into training and testing datasets based on the model architecture and nature of the study. The dataset can be randomly split for training, validation, and testing or based on the number of subjects and trials. According to the study, splitting ratios can be chosen heuristically, with common ratios being 70–20–10 or 80–10–10 for training, validation, and testing, respectively (Mundt et al., 2020; Xia et al., 2020). Considering CNNs, data is presented as a collection of images/matrices based on batch size and time structure (Hajian et al., 2021; Yu et al., 2022; Zhang, Fragnito et al., 2022). For other architectures, dataset rows represent time-series entries, and columns represent features (Su et al., 2020; Wang et al., 2023). Overall, the quantity, quality, and variety of training data play a significant role in model performance and the generalizability of the developed networks to a population outside the training sample. Test datasets also need to be representative of a subject population to effectively evaluate a neural network's performance.

Data may also be segmented into time-slices through windowing, which allows for a memory component (LSTMs) and a continuous future torque trajectory estimation by sliding across the windows (Liu et al., 2009; Su et al., 2020; Wang et al., 2023; Zhang, Soselia et al., 2022). Studies with a variety of features also employed data augmentation techniques such as feature scaling or normalisation (Lim et al., 2019), which is on par with dimensionality reduction. High dimensional datasets may incur the curse of dimensionality, leading to increased computational load, overfitting, and difficulties in interpretation and visualisation. Accordingly, techniques such as principal component analysis (PCA) reduce the number of features while retaining relevant information in the dataset, which enhances computational efficiency (Yu et al., 2022).

Evaluation Metrics

In literature, the actual upper and lower limb torques are derived using sensors (load cells) or an ID approach via Mocap data (Figure 3). The Newton-Euler Equation 1 of motion for joint torque is used and commonly computed through biomechanical analysis software such as OpenSim. An unseen portion of data is used for testing with error and correlation evaluation metrics to determine the performance of a model. It includes root mean square error (RMSE), normalised RMSE (NRMSE), and relative RMSE (RRMSE), which quantify the error between the actual and predicted joint torques (Siu et al., 2021). Correlation coefficients (R) such as Spearman's or Pearson's are derived and highlight the similarity in fit or trend between the actual and predicted torques. Pearson's is commonly seen in literature, while Spearman's is also applicable considering the monotonic relationship between predicted and actual torques (Liu et al., 2019; Moreira et al., 2021). Additionally, the coefficient of determination (R^2) measures how well the neural network replicated the actual torques (Truong et al., 2023). Yet, it is challenging to directly compare neural network performance across studies. It is due to varying experimental setups, test datasets, validation methods, model architectures (including hyperparameters) and, in some instances, the lack of standardised evaluation metrics (Naidu et al., 2023). Hence, establishing common benchmarks for joint torque prediction (such as using gold standard Mocap with an RMSE metric) is necessary to allow comparability of results.

$$M(q) \cdot \ddot{q} + C(q, \dot{q}) \cdot \dot{q} + G(q) + \mathrm{F} = \tau \quad [1]$$

Where $\tau \in R$ is the vector of generalised torques, $M(q)$ is the system mass matrix, $C(q, \dot{q})$ is the vector of Coriolis and centrifugal forces, $G(q)$ is the vector of gravitational forces, and F is the vector of external forces. The generalised vectors of position, velocity and acceleration are represented by $q, \dot{q},$ and $\ddot{q}$, respectively (Truong et al., 2023).

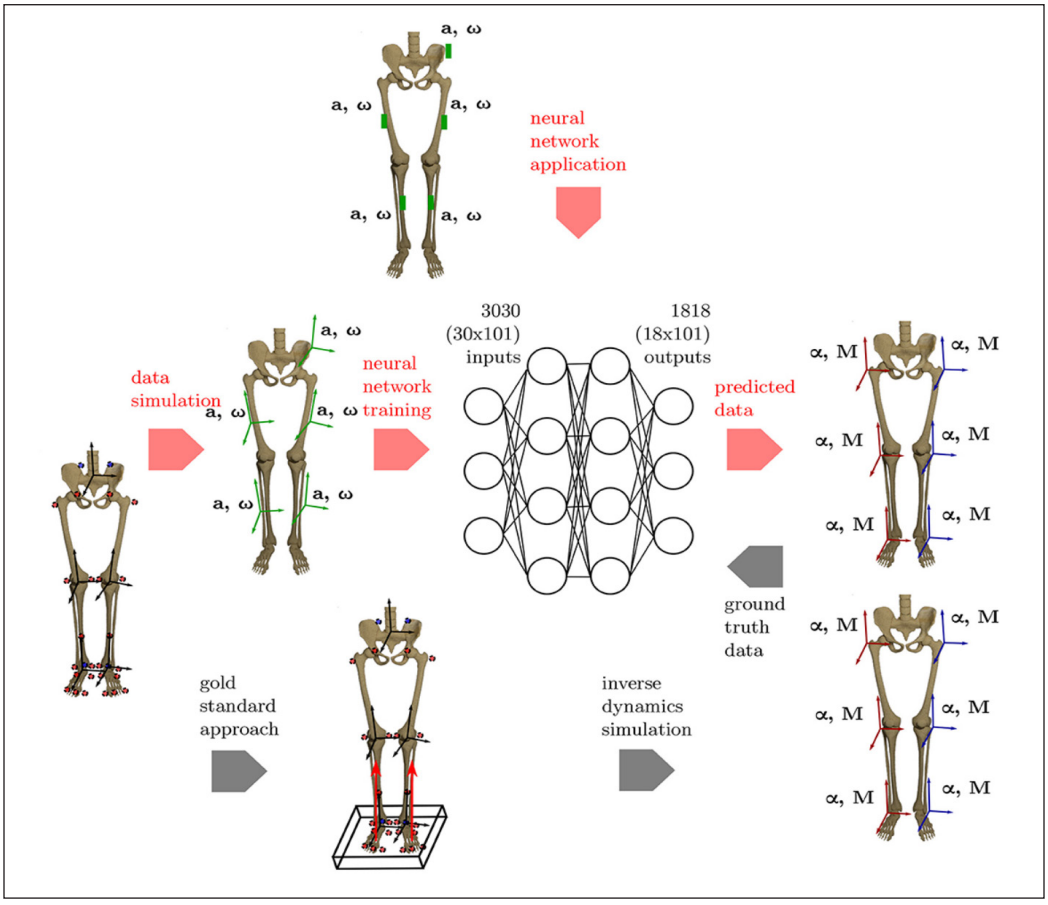

Figure 3. Training of a neural network where ground truth values are calculated using an inverse dynamics approach, with data from an optical motion capture system and force plates. Reprinted and modified with permission from (Mundt et al., 2020) and published under the Creative Commons Attribution License (CC BY 4.0)

Neural Network Architectures

Artificial Neural Networks

Molinaro et al. (2020) developed a feedforward neural network to estimate hip torque using hip joint angles, thigh acceleration, and angular velocity as inputs from a single thigh IMU. The dataset contained five extracted features (minimum, maximum, mean, standard deviation and latest values) and was segmented into temporal windows of 350 ms. The trained network consisted of three hidden layers with 30 neurons and an exponential linear unit activation function. The model was trained under two conditions where the ambulation mode (gait or ramp ascent/descent) was known or unknown. At the same time, an early stop based on validation loss was implemented to prevent overfitting or underfitting. On average, the ANN produced an RMSE of 0.116 Nm/kg, with a 59.3% reduction compared to

a mathematical model using a mean torque profile. The study showed that ANNs produced better estimates of joint torque compared to mathematical approximations and highlighted the need for a classifier to distinguish between the different movements. Similarly, Mundt et al. (2020) used IMU accelerations and angular velocities of the lower limbs (five sensors) to predict hip, knee, and ankle torque in all motion planes. Synthetic IMU data was created using optical Mocap. At the same time, their ANN had a higher complexity with two hidden layers consisting of 6000 and 4000 neurons, respectively, followed by a 40% dropout rate and 15,000 training steps. The final network had an R of 0.95 and an NRMSE of less than 13%.

Lim et al. (2019) used COM kinematics to predict lower body joint torques, joint angles, and GRF (Figure 4). A single Sacrum IMU obtained COM data, and the study investigated which kinematic features amongst acceleration, velocity, displacement, and time contributed the most to performance. Hence, models were trained using combinations of these inputs where the ANN had a single hidden layer with 20 neurons and a sigmoid activation function. COM displacement was found to be the most significant contributor, where omission of this input increased error by up to 3%. The hip, knee, and ankle had NRMSE percentages of 10.74, 9.63 and 9.24, respectively, with R greater than 0.90. Chandrapal et al. (2011) used SEMG from five knee flexor/extensor muscles to create a direct mapping to knee joint torque. The ANN consisted of a single hidden layer with five neurons, and the lowest average error was 10.46%. However, this network is only considered a single subject and may not be generalisable to other individuals.

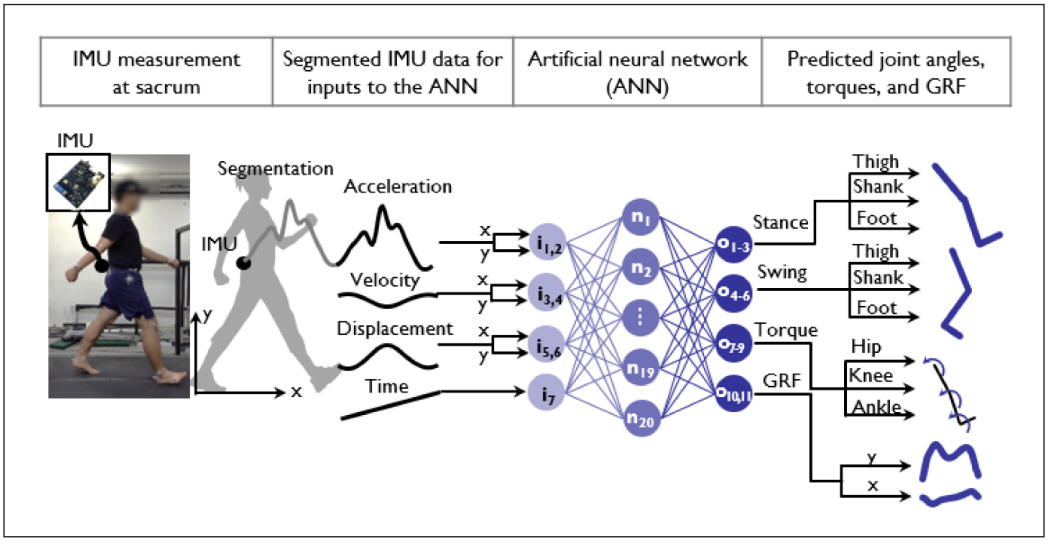

Figure 4. An artificial neural network (ANN) architecture for predicting hip, knee, and ankle joint torques using the centre of mass kinematics obtained from a single Sacrum inertial measurement unit (IMU) sensor. Reprinted with permission from (Lim et al., 2019) and published under the Creative Commons Attribution License (CC BY 4.0)

Moreover, Liu et al. (2009) proposed using GRFs to predict hip, knee, and ankle torques during jumping and squatting. Their ANN consisted of a single hidden layer with 10 neurons and a sigmoid activation function, and the input features were time histories of vertical GRF, vertical displacement, COM velocity, jump power, and support time. The model produced an R greater than 0.95 and relative percentage errors of 4.73, 2.13 and 6.33 for the hip, knee, and ankle, respectively. This study showed the applicability of ANNs in predicting the non-linear relationship between GRF and torque. Likewise, McCabe et al. (2023) extended this research by including IMU data with GRF from insoles (wearable sensors) for estimating hip torque during stair ascent. Their model had two hidden layers, each with 10 neurons and a hyperbolic tangent (Tanh) activation function sensitive to high variability inputs. The trained network had an RRMSE of 17.8% with an R^2 of 0.77.

Time Delay Neural Networks

As Su et al. (2020) presented, TDNNs typically consist of a fully connected ANN structure with a time delay (Figure 5). SEMG inputs are utilised as they generate 30 to 150 ms before muscle movement or motion onset. This study predicted ankle inversion/eversion torque with input features being ankle angular velocity and a 100-point RMS moving window with a 30-sample overlap of the SEMG signal of five lower body muscles. The TDNN consisted of a single hidden layer with 10 neurons and a sigmoid activation function, resulting in an NRMSE of 7.9% and an R of 0.97. This model outperformed an ANN and a support vector regression (SVR) model (NRMSE of 9.8% and 9.07%, respectively), showcasing its applicability to time series prediction. Similarly, Peng et al. (2015) developed a

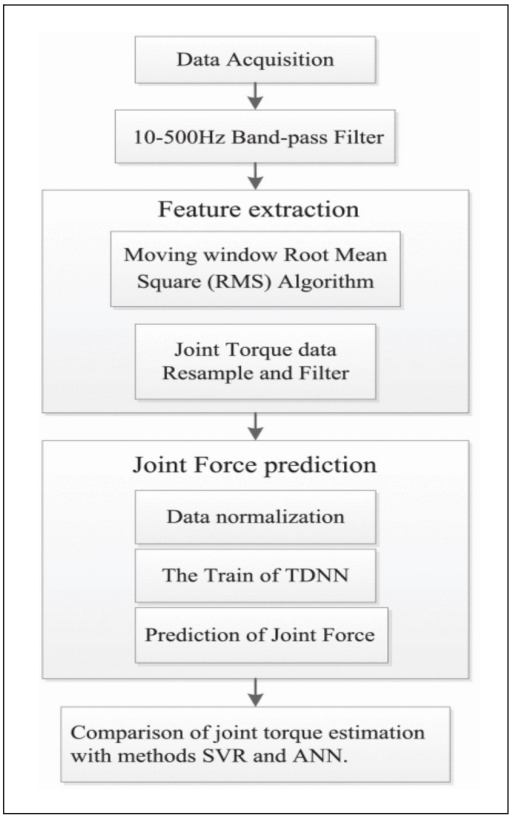

Figure 5. (a) The procedure for ankle joint torque prediction, and (b) the network structure for a time delay neural network (TDNN). Reprinted with permission from (Su et al., 2020) and published under the Creative Commons Attribution License (CC BY 4.0)

TDNN for estimating elbow torque using joint angles, angular velocity, and a 200 ms moving average window of the SEMG signals from two arm muscles. The model had a single hidden layer with 25 neurons, producing an RMSE of 0.60. Additionally, this study conducted a zero-EMG test, where the SEMG signals were omitted as inputs during training. In this instance, torque prediction was almost zero, showing the importance of SEMG to this neural network architecture with a lower dependence on kinematic parameters.

Convolution Neural Networks

Moreira et al. (2021) compared the performance of a CNN and LSTM when predicting ankle torque during gait, tailored to the subject's walking speed and anthropometry. The authors also tested non-SEMG dependent torque estimation accuracy, as SEMG sensors are affected by noise from muscle crosstalk, skin-electrode displacement, sweat or temperature and, therefore, are not ideal for long-term operation in wearable devices. Two types of models were trained where the first model had inputs of ankle angle, angular velocity, acceleration, walking speed, height, mass, foot and shank length, gender, and age. The second model had SEMG signals added for two shank muscles. The CNN architecture had two convolution layers with 8–16 filters, a 2x2 kernel size and a 25% dropout, while the LSTM had a single layer with 100 neurons and a 50% dropout. Overall, the CNN outperformed the LSTM, where NRMSE, Spearman's R and R^2 were 0.7% against 0.58%, 0.89 against 0.84 and 0.91 against 0.79 for the CNN and LSTM, respectively. Moreover, the CNN had a faster prediction time of 0.51 ms/sample compared to 3.7 ms/sample for the LSTM.

Thus, the study highlighted the importance of torque prediction, oriented towards the user's anthropometry and speed, for personalised and more effective applications. The results showed no significant differences between CNN and LSTM models with and without SEMG signals as inputs. It justifies that SEMG is unnecessary for torque prediction in these architectures, and joint kinematics are sufficient. It is further supported by Hajian et al. (2021), where elbow torque was predicted using only SEMG and then SEMG with position and velocity from a Biodex machine. Their CNN had two convolution layers with 16 and 64 filters, a 3x3 kernel size, followed by normalisation, rectified linear unit (ReLU) activation, pooling, and dense layers. Results showed improved R^2 by percentages of 2.35, 37.50 and 16.67 when SEMG and position were used, compared to only SEMG for isotonic, isokinetic, and dynamic movement conditions, respectively. R^2 then increased by further percentages of 2.29, 12.2 and 20.50 when velocity was added for the same isotonic, isokinetic, and dynamic cases, respectively.

Further, Zhang, Fragnito et al. (2022) evaluated the CNN performance of two models for ankle torque estimation, with the first using brightness mode ultrasound images of muscles and the second using SEMG from the shank muscles as inputs (Figure 6). It was performed using ultrasound transducers with similar regions of interest for both types of inputs during

gait. Unlike SEMG, ultrasound imaging produces a direct muscle visualisation, a high signal-to-noise ratio, and no explicit feature extraction is needed. Instead, a direct mapping to ankle torque is produced. A seven-layer convolution architecture containing conv2D and pooling layers with batch normalisation and ReLU activation was used. A 3x3 kernel size was used, with the first and second convolution layers having eight and 16 filters, followed by 32 filters for the rest. This study showed that CNNs utilising ultrasound imaging had improved performance to SEMG inputs, with a reduction in NRMSE by 37.55% and an increase in R^2 by 20.13%. Likewise, Yu et al. (2022) also used SEMG signals as images for

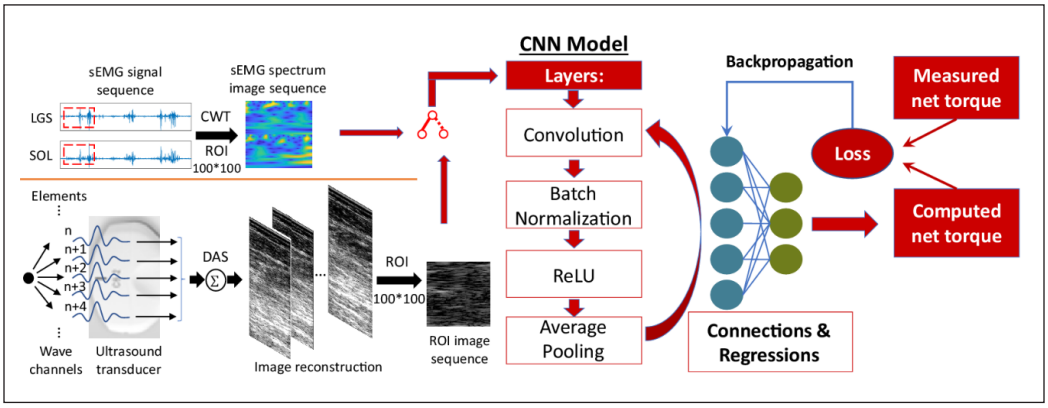

(a)

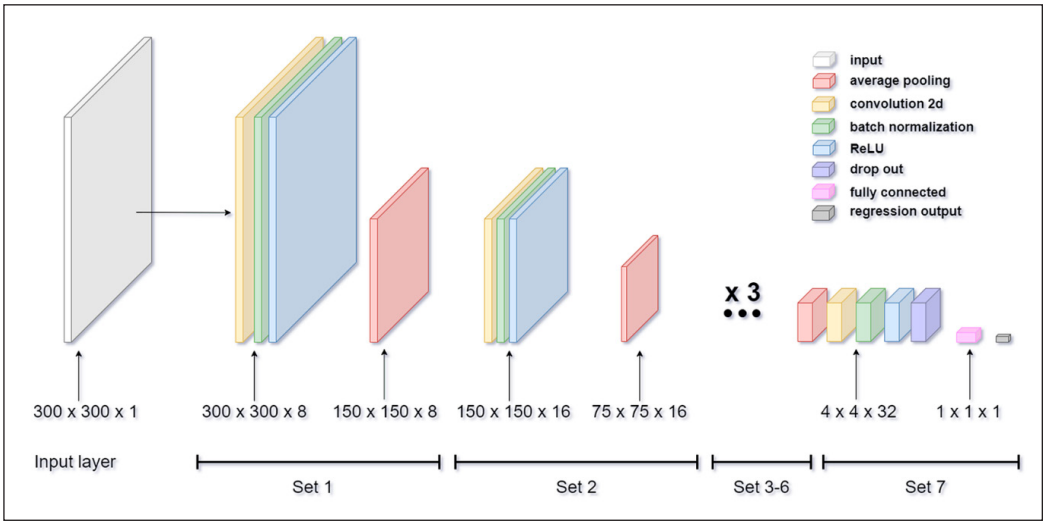

(b)

Figure 6. (a) An overview of the data collection, preprocessing, and training steps for a convolution neural network (CNN) using ultrasound images of muscles as inputs. (b) The developed CNN architecture with individual layers, where the layer output size depends on the region of interest (300 x 300 pixels) from the ultrasound images. Reprinted with permission from (Zhang, Fragnito et al., 2022) and published under the Creative Commons Attribution License (CC BY 4.0)

predicting wrist torques. These signals were converted into 2D arrays based on electrode positioning to form a collection of input images at every sampling instant, while PCA was used for dimensionality reduction. The CNN architecture had six convolution layers (filter sizes were 16, 64, 64, 64, 64 and 16) with batch normalisation, ReLU and pooling layers, a 3×3 kernel size, and a 10% dropout. Relatively good performance was seen in comparison to three regressive models and a short-time Fourier transform CNN, where R was 0.95 and 0.96, and NRMSE was 7.9% and 6.8% for pronation/supination and flexion/extension wrist torques, respectively.

Alternatively, for time series analysis, 1D CNNs can be used, as presented by Ozates et al. (2023), for hip, knee, and ankle torque prediction. Inputs were lower body and trunk joint angles in sagittal, coronal, and transverse planes, which can be easily measured using wearable sensors and remove the need for costly Mocap equipment. This model was trained for typically developed individuals and patients with Cerebral Palsy. The 1D-CNN had five convolution layers (filter sizes of 128, 128, 512, 1024 and 2048) with five kernel sizes (30, 15, 10, 5, 3) along with flattening and 10 densely connected layers, with neurons ranging from 10000 to 100. Results showed NRMSE between 18.02%–13.58% and 12.55%–8.5%, while R was between 0.85–0.93 and 0.94–0.98 for Cerebral Palsy and typically developed subjects, respectively. Model performance was greater for typically developed subjects with lower NRMSE and higher correlation. Cerebral Palsy patients had larger gait deviations, which produced a more complex mapping from joint angle to torque, resulting in reduced performance.

Long Short-term Memory Neural Networks

Zhang et al. (2023) presented an LSTM neural network (Figure 7) for predicting hip, knee, and ankle torques and compared its performance with an NMS model. Inputs were SEMG and joint angles taken as time slice data with a t-distributed stochastic neighbour embedding algorithm for dimensionality reduction. Alternatively, the NMS model was created using the CEINMS toolbox, which derives joint torque from SEMG. Both models were trained under three conditions: (1) pooled, (2) individual, and (3) clustered. Pooled data from 10 movements was used to train a single NMS and LSTM model, while individuals used each subject's data per model, and clustered training grouped similar movements together. Clustering was performed using K-means, and a single group included movements like slow, normal, and fast walking. The LSTM consisted of 50 neurons, a Tanh activation function, and a dense layer of 64 neurons. Overall, the LSTM showcased better performance than the NMS model, where NRMSE for LSTM and NMS were less than 6.7% and less than 19.3%, respectively. The study also found that clustering did not improve LSTM accuracy but did so for NMS modelling, which shows that clustered motions have similar coordination patterns. On par with clustering, Zhang, Soselia et al. (2022) also proposed

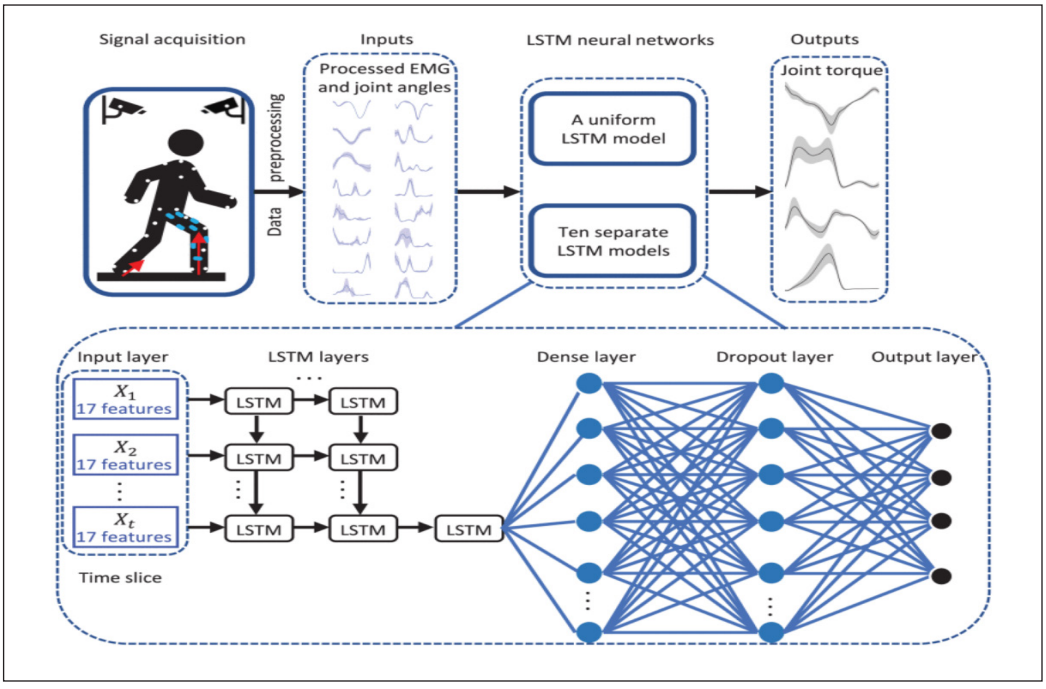

(a)

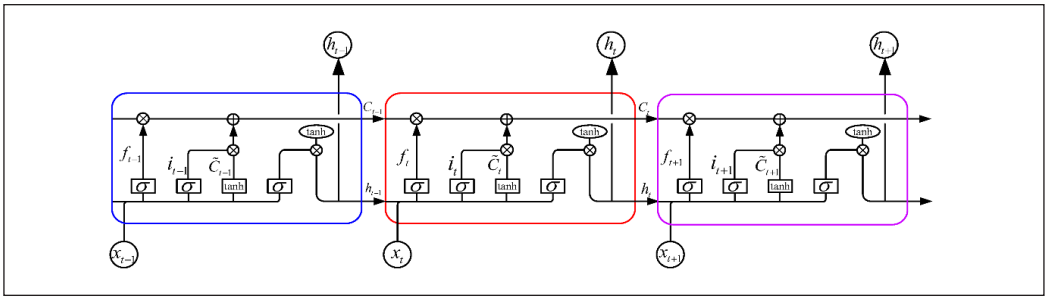

(b)

Figure 7. (a) Overview of a long short-term memory (LSTM) neural network architecture for estimating hip, knee, and ankle joint torque. Two models were developed where (1) a uniform LSTM was trained with data from multiple tasks and (2) 10 separate LSTM models were trained for each task. Reprinted with permission from (Zhang, Soselia et al., 2022) and published under the Creative Commons Attribution License (CC BY 4.0). (b) The gated structure of an LSTM network, with forget, input, and output gates, followed by memory and hidden cell states. Reprinted with permission from (Wang et al., 2023) and published under the Creative Commons Attribution License (CC BY 4.0)

a transfer learning method where a similar LSTM was pre-trained on multiple subjects/ movements (generalised model) and then transferred its knowledge to a target subject or motion. The model can learn new tasks faster if it has learnt similar knowledge, notably with limited data. Hence, a collection of LSTMs was developed for inter- and intra-subject tasks, with some models trained on all 10 tasks or 10 separate LSTMs for each motion.

Overall, RMSE was less than 0.14 Nm/kg, with significant improvements in performance once transfer learning was implemented.

Siu et al. (2021) designed an LSTM for mapping both instantaneous and sequences of ankle torque from SEMG and IMU data, with comparison to an ANN, CNN, and neural ordinary differential equation. The input data was split into historical windows of 0.5 s with a 0.49 s overlap. The LSTM had a single hidden layer with 64 neurons, two dense layers with 16 neurons each and a leaky ReLU activation function. RMSE and R for all activities were 0.08 Nm/kg and 0.88 for the LSTM, in comparison to 0.10 Nm/kg and 0.80 for the CNN. This study highlighted the superior performance of the LSTM for time series estimation. Similarly, Wang et al. (2023) developed a three-layer LSTM network (32, 16 and 8 neurons) with time-sliced input data forming a 150 ms window for time domain features and a 128 ms window for frequency domain features. The inputs themselves were five SEMG signals and three joint angles (lower body) for predicting hip, knee, and ankle torques. The model performance was compared against a Gaussian process regression model, which showed NRMSE to be less than 15% and R to be greater than 0.85. Truong et al. (2023) also produced a two-layer stacked LSTM using a collection of input features extracted from SEMG to predict knee and ankle torques. Mean R^2 for the knee and ankle torques were 94.9% and 85.44%, respectively. At the same time, the study further supported that LSTMs are currently the optimal architecture for time series torque prediction as they remember and employ temporal dependencies.

Hybrid Neural Networks

Considering joint torque estimation, hybrid networks predict alternate biomechanical parameters, which are then used in computational NMS or mathematical models to calculate torque (Figure 8). For instance, Dinovitzer et al. (2023) used joint angles, body segment positions, velocities, and accelerations through an ANN to generate GRF and ZMP output trajectories. These were then combined with joint kinematics into a dynamical mathematical model to derive hip, knee, and ankle torques. Parallelly, an end-to-end ANN was trained for comparison, with direct torque mapping from the joint kinematic inputs. The hybrid ANN had two hidden layers of 20 and 10 neurons and used a Tanh activation function.

Significant differences in performance were observed for the hip and knee, but not the ankle, with better accuracy from the hybrid model than the end-to-end ANN, noting that only a small sample size (n=11) was used. The hybrid model has superior generalizability to varying conditions from the training data, such as when using an assistive device which changes subject mass distribution. As such, this model was further tested on a single subject wearing an exoskeleton (Indego, Parker Hannifin, USA), where R was greater than 0.84 and 0.59 for the hybrid and end-to-end ANN, respectively. Comparably, Lam and Vujaklija (2021) developed a similar model where an ANN predicted GRF and COP and then derived

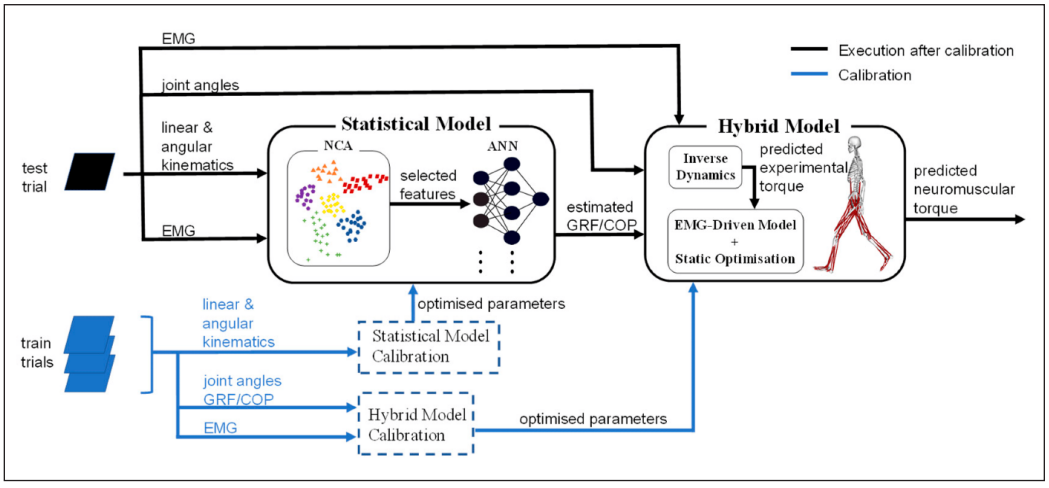

Figure 8. Overview of a hybrid neural network consisting of data collection, preprocessing and an ANN to estimate ground reaction force (GRF) and centre of pressure (COP) features. It also contains a hybrid neuromusculoskeletal (NMS) model, which uses the predicted kinetics as inputs to computationally derive joint torque. Reprinted with permission from (Lam & Vujaklija, 2021) and published under the Creative Commons Attribution License (CC BY 4.0)

joint torque through NMS modelling. Results showed RMSE less than 0.15 Nm/kg and R greater than 0.70. The reasoning behind these models is to remove the need for bulky and costly Mocap lab equipment like force plates when performing NMS analysis.

Schulte et al. (2022) presented a hybrid CNN-NMS model for multi-day estimation of knee torque. Three models were trained: (1) CNN for direct SEMG to torque mapping, (2) NMS modelling using SEMG (OpenSim via Gait2392 and Hill-type musculoskeletal models) and (3) a hybrid model where a CNN maps SEMG to muscle activation, which a NMS model uses to derive knee torque. The CNN architecture consisted of three 1D convolution layers (32 filters), batch normalisation and ReLU activation, followed by a single LSTM layer (64 neurons), a dense layer and dropout. Overall, the CNN model produced the best performance with NRMSE of 9.2%, followed by the hybrid and NMS models with NRMSE of 12.4% and 14.3%, respectively. Likewise, Wang and Buchanan (2002) also developed a hybrid ANN that maps SEMG to muscle activation, followed by an NMS model to estimate elbow joint torque. Their ANN contained two hidden layers (10 and 15 neurons) and used normalised SEMG of 10 upper body muscles. At the same time, average relative errors for isometric flexion were 4.9% for ramping up/down to relaxation and 34.2% for cycles (larger error as motion differed from training data).

Alternate Network Architectures

Apart from ANNs, CNNs, and LSTMs, alternate architectures were proposed for joint torque estimation that utilised combinations of these networks (Figure 9). Ardestani et

al. (2014) used a wavelet neural network, an ANN where the hidden layer has wavelet activation functions (Tansig and Purlin), to consider inputs in time and frequency domains. These functions use a Morlet mother wavelet, and inputs were eight SEMG and two GRF signals. Hip, knee, and ankle torque estimation were compared between a traditional ANN and the wavelet network, which produced better results with NRMSE less than 10% and R greater than 0.94. Huang et al. (2020) employed autoencoders from SEMG for feature

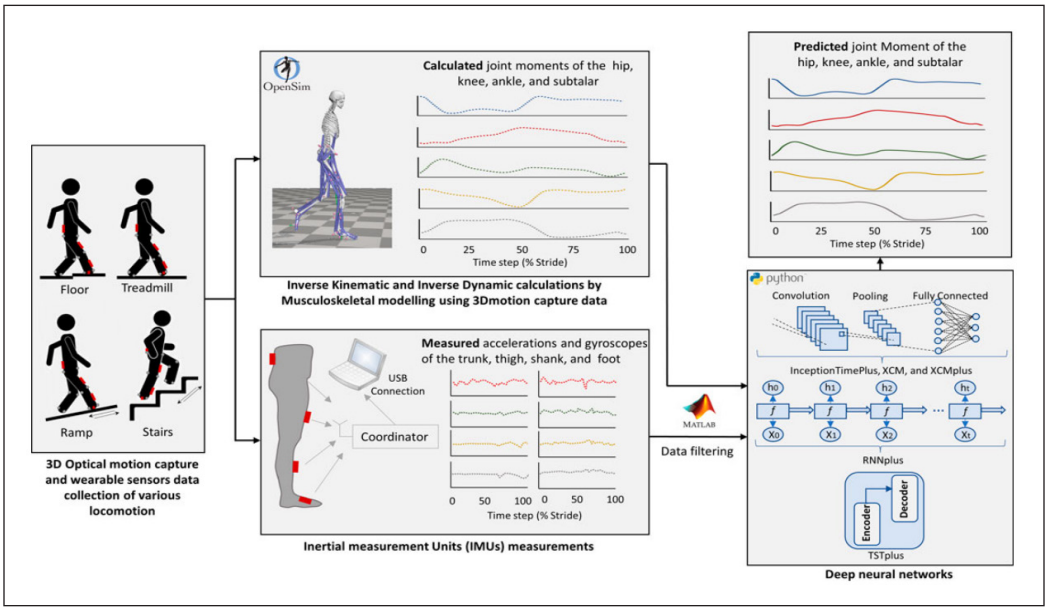

(a)

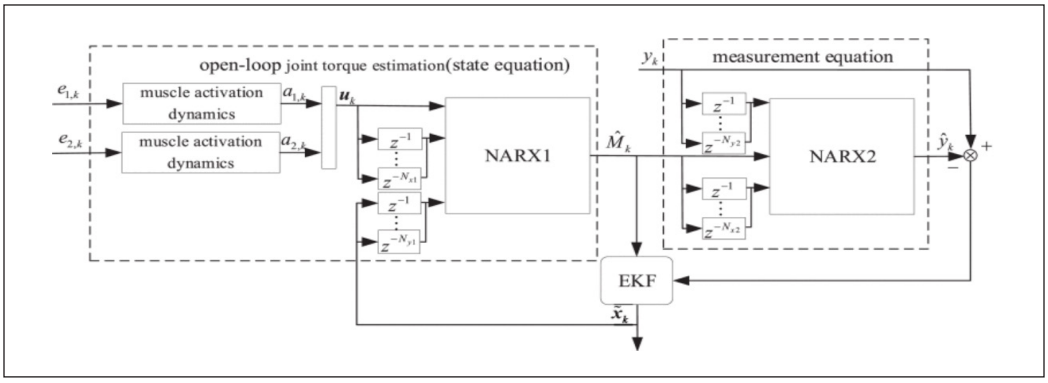

(b)

Figure 9. (a) Overview of the data collection, preprocessing and network architecture for a convolution neural network, InceptionTimePlus, explainable convolution (XCM), XCMplus, RNNplus and Time series transformer (TSTplus). Reprinted with permission from (Altai et al., 2023) and published under the Creative Commons Attribution License (CC BY 4.0). (b) A closed-loop controller using two non-linear autoregressive with exogenous input (NARX) neural networks for joint torque and angle estimation. Reprinted with permission from (Li et al., 2020) and published under the Creative Commons Attribution License (CC BY 4.0)

selection and shoulder and elbow torque trajectory generation. The autoencoders had three hidden layers with a Tanh activation function, while this result was fed into an ANN, producing an RMSE of 1.38 Nm/kg and an R of 0.94.

Altai et al. (2023) further trained multiple models using IMU data to predict hip, knee, and ankle torques (Figure 9). The models were (1) InceptionTimePlus, (2) explainable convolution (XCM), (3) XCMplus, (4) RNNplus and (5) Time series transformer (TSTplus). InceptionTimePlus is made of 1D CNN layers, while XCM uses 2D convolutions for feature extraction and 1D convolutions for extracting temporal information in time series interactions. XCMplus builds on XCM by keeping the 2D and 1D convolutions in sequence, while RNNplus contains a conv1D layer with a stacked LSTM architecture. Finally, TSTplus uses an encoder-decoder transformer for probabilistic forecasting. The results showed that XCM was the optimal model with an average RMSE of 0.046 compared to 0.064 from the other models. Moreover, Li et al. (2020) discussed using a non-linear autoregressive with exogenous inputs (NARX) neural network for real-time elbow torque estimation within a closed-loop controller. Muscle activation was derived from SEMG data and inputted into the network to produce joint torque. NARX consisted of a multi-layer feedforward network with a single hidden layer (5 neurons) and a Tansig activation function, which allows for highly non-linear mapping with noisy data. For the controller, two NARX models were implemented, where the first estimates joint torque, and the second uses this successively to estimate joint angle trajectories. It is run through a Kalman filter to create a closed-loop model, where joint angles are reused as inputs in the first NARX network.

DISCUSSION

This review focuses on neural networks that estimate upper and lower body joint torques for use with wearable technology. Torque trajectory generation is a necessary step in designing the control systems for assistive devices, in rehabilitation or to support impairment (Dinovitzer et al., 2023; Li et al., 2020; Siu et al., 2021; Wang et al., 2023). Healthy adult torque trajectories are a baseline for assessing impaired motion and ensuring sufficient assistive torque is supplied based on a patient's requirements. This produces a natural and effective application of aid from assistive devices (Moreira et al., 2021; Perera et al., 2023).

Compared to conventional methods of torque estimation (ID, mathematical and NMS models), neural networks offer distinct advantages which are valuable for integration with wearable technology. Once trained, they streamline the estimation process by directly mapping sensor input (for example, SEMG, GRF or IMU) to output torque while reducing the need for tedious modelling, calibration, and processing of data from individual subjects (Lim et al., 2019; Schulte et al., 2022; Wang & Buchanan, 2002). Neural networks can also provide personalised torque trajectories for each user based on age, anthropometry,

biological sex, or movement speeds. It allows for user-oriented assistive torque compared to generic levels of assistance from traditional methods like mathematical modelling (Moreira et al., 2021). Future research could expand on this by generating personalised torque trajectories based on movement execution strategies or styles for a more natural application of assistance (Perera et al., 2023). However, it is imperative to acknowledge the limitations of neural networks. The black box nature of these models limits the understanding of the relationships and estimation methods behind their torque prediction, while model performance is highly dependent on the quality and quantity of the training data (Liu et al., 2009; Siu et al., 2021). Models would also need to be re-trained when used for specific movement impairments or if user characteristics greatly differ from the trained subject data (Molinaro et al., 2020).

Existing literature, as reviewed, predicted torques with low errors - RMSE and NRMSE less than 1.4 Nm/kg and 15%, respectively, and strong correlation coefficients greater than 0.84. LSTMs produced strong instantaneous sequential torque estimates (Siu et al., 2021) for multiple movements through pretraining on a range of tasks and transferring this knowledge to a target subject (Zhang, Soselia et al., 2022). Other networks produce tailored torque trajectories by accounting for subject characteristics (Moreira et al., 2021) or through NMS modelling (Dinovitzer et al., 2023). However, most studies had small sample sizes ($n<10$, Table 1), which is statistically acceptable (Lim et al., 2019; Molinaro et al., 2020; Peng et al., 2015; Zhang et al., 2023) but pose a challenge in generalising neural networks to a population. Future studies should incorporate larger datasets ($n>30$, considering the central limit theorem) encompassing wide age groups, subject anthropometries, characteristics, and movement strategies to account for population variance (Moreira et al., 2021; Perera et al., 2023). Moreover, models trained to estimate torque for multiple movements suffered a drop in performance. Therefore, future research should investigate the applicability and real-time capability of training multiple models for individual motions or a single model for multiple motions. Training techniques incorporating clustering (grouping similar movements) or transfer learning (leveraging pre-trained models to expedite training for new movements) can be explored as possible solutions (Zhang, Soselia et al., 2022; Zhang et al., 2023). Neural networks for torque estimation form the mid-level control component in assistive devices (Liu et al., 2019). They need to work hand-in-hand with high-level controllers for motion classification and intention detection, which would trigger the assistive device. Future work should combine these systems in real-time to improve applications for multiple movements and form an overall control architecture (Molinaro et al., 2020).

In the context of wearable devices, kinematic, kinetic or SEMG signals (from appropriate muscles) are required as inputs into the neural networks for estimating the targeted joint torques. Selections on model architecture (ANN, CNN, LSTM, or hybrid)

and data preprocessing techniques such as filtering, scaling, or normalisation also need to be made. With this, the dataset needs to be split for training, testing, and validation (for example, a 70%–20%–10% split) with appropriate test methods based on the type of prediction (Mundt et al., 2021). Joint torque estimation commonly follows time series data, where walk-forward or cross-validation methods can be used depending on sequence, instantaneous, or windowed outputs (Siu et al., 2021; Yu et al., 2022). Furthermore, hyperparameter tuning is specific to each network and dataset. While there is potential for reusing training parameters from a holistic perspective, their adaptability depends on the model architecture, inputs, outputs and data characteristics. Accordingly, larger networks with more hidden layers and neurons tend to produce closer torque estimations with lower error but also require longer computation time and resources and result in slower real-time operation (Ozates et al., 2023; Truong et al., 2023).

Consideration for the optimal input parameters for joint torque estimation involves evaluating the biomechanical quantities used. While ID methods using Mocap and GRFs present the gold standard approach to torque estimation, their reliance on expensive and bulky laboratory equipment reduces portability and is not easily adopted by wearable technology (McCabe et al., 2023; Siu et al., 2021). SEMG is advantageous as it precedes muscle movement but faces issues due to noise, muscle crosstalk, sensor placement, electrode-skin displacement, sweat and temperature, making prolonged wear difficult (Su et al., 2020). Additionally, ultrasound muscle imaging captures detailed information for personalised torque estimation but produces noisy data, requires tedious preprocessing and is highly dependent on sensor placement (Zhang, Fragnito et al., 2022). Thus, the ideal inputs are kinematic parameters such as joint angles, angular velocities, and accelerations. These can be efficiently acquired from wearable sensors like IMUs or encoders, ensuring easy integration with wearable technology. Moreover, across the literature, the number of IMUs (wearable sensors) utilised varied, with certain studies using just a single IMU to accurately estimate joint torque (Lim et al., 2019; Molinaro et al., 2020). The performance of all networks was comparable ($R>0.85$ and error$<20\%$), highlighting that the location of placement is a significant contributor to torque estimation compared to the number of sensors used (Höglund et al., 2021).

In comparison with the reviewed network architectures, CNNs and LSTMs produced the best overall performance for joint torque estimation. Moreira et al. (2021) stated that CNNs had a smaller computation time and better performance than LSTMs. However, Siu et al. (2021) argued that LSTMs outperform CNNs, with both studies considering SEMG inputs. Therefore, both architectures are deemed optimal as they capture the spatial and temporal dependencies when mapping inputs to output torque. They are well suited for time-series forecasting, incorporating time slices (sliding windows) for real-time operation (Wang et al., 2023; Zhang et al., 2023). Hence, an example of an architecture that could

be further investigated is the CNN-LSTM, which combines both models to capture spatial and temporal characteristics. Further research is also needed on optimal window sizes for real-time applications and techniques to minimise the burn-in time of LSTMs, as the first few values are considered for memory (Siu et al., 2021).

CONCLUSION

The study reviewed existing literature on neural networks for upper and lower limb joint torque estimation, covering diverse architectures such as ANNs, TDNNs, CNNs, LSTMs, hybrid, wavelet, NARX, and autoencoders. From this, joint kinematics were identified as optimal inputs for torque estimation in wearable devices. CNNs and LSTMs are the current optimal models for time series estimation due to their proficiency in learning spatiotemporal dependencies. Future work should prioritise larger sample sizes, more inclusive datasets, and the development of models for real-time applications. Torque estimation neural networks should also work on par with motion classifiers for intention detection and prediction of joint torque for multiple movements.

ACKNOWLEDGEMENT

This work is supported by the Ministry of Higher Education, Malaysia, under the project number FRGS/1/2022/TK07/MUSM/02/2.

REFERENCES

Altai, Z., Boukhennoufa, I., Zhai, X., Phillips, A., Moran, J., & Liew, B. X. W. (2023). Performance of multiple neural networks in predicting lower limb joint moments using wearable sensors. *Frontiers in Bioengineering and Biotechnology*, *11,* Article 1215770. https://doi.org/10.3389/fbioe.2023.1215770

Ardestani, M. M., Zhang, X., Wang, L., Lian, Q., Liu, Y., He, J., Li, D., & Jin, Z. (2014). Human lower extremity joint moment prediction: A wavelet neural network approach. *Expert Systems with Applications*, *41*(9), 4422–4433. https://doi.org/10.1016/j.eswa.2013.11.003

Chandrapal, M., Chen, X., Wang, W., Stanke, B., & Pape, N. L. (2011). Investigating improvements to neural network based EMG to joint torque estimation. *Paladyn*, *2*(4), 185–192. https://doi.org/10.2478/s13230-012-0007-2

Cho, K., Merrienboer, B. V., Gulcehre, C., Bahdanau, D., Bougares, F., Schwenk, H., & Bengio, Y. (2014). *Learning phrase representations using RNN encoder-decoder for statistical machine translation*. arXiv. https://doi.org/10.48550/arXiv.1406.1078

Crenna, F., Rossi, G. B., & Berardengo, M. (2021). Filtering biomechanical signals in movement analysis. *Sensors*, *21*(13), Article 4580. https://doi.org/10.3390/s21134580

Delp, S. L., Anderson, F. C., Arnold, A. S., Loan, P., Habib, A., John, C. T., Guendelman, E., & Thelen, D. G. (2007). OpenSim: Open-source software to create and analyze dynamic simulations of movement. *IEEE Transactions on Bio-Medical Engineering*, *54*(11), 1940–1950. https://doi.org/10.1109/TBME.2007.901024

Dinovitzer, H., Shushtari, M., & Arami, A. (2023). Accurate real-time joint torque estimation for dynamic prediction of human locomotion. *IEEE Transactions on Biomedical Engineering*, *70*(8), 2289-2297. https://doi.org/10.1109/TBME.2023.3240879

Farina, D., & Enoka, R. M. (2023). Evolution of surface electromyography: From muscle electrophysiology towards neural recording and interfacing. *Journal of Electromyography and Kinesiology*, *71*, Article 102796. https://doi.org/10.1016/j.jelekin.2023.102796

Hajian, G., Morin, E., & Etemad, A. (2021, November 1-5). *Convolutional neural network approach for elbow torque estimation during quasi-dynamic and dynamic contractions*. [Paper presentation]. 43rd Annual International Conference of the IEEE Engineering in Medicine and Biology Society (EMBC), Mexico City, Mexico. https://doi.org/10.1109/EMBC46164.2021.9630287

Höglund, G., Grip, H., & Öhberg, F. (2021). The importance of inertial measurement unit placement in assessing upper limb motion. *Medical Engineering & Physics*, *92*, 1–9. https://doi.org/10.1016/j.medengphy.2021.03.010

Huang, Y., Chen, K., Zhang, X., Wang, K., & Ota, J. (2020). Joint torque estimation for the human arm from sEMG using backpropagation neural networks and autoencoders. *Biomedical Signal Processing and Control*, *62*, Article 102051. https://doi.org/10.1016/j.bspc.2020.102051

Kruk, E. V. D., Strutton, P., Koizia, L. J., Fertleman, M., Reilly, P., & Bull, A. M. J. (2022). Why do older adults stand-up differently to young adults? Investigation of compensatory movement strategies in sit-to-walk. *Npj Aging*, *8*(1), Article 13. https://doi.org/10.1038/s41514-022-00094-x

Lam, S. K., & Vujaklija, I. (2021). Joint torque prediction via hybrid neuromusculoskeletal modelling during gait using statistical ground reaction estimates: An exploratory study. *Sensors*, *21*(19), Article 6597. https://doi.org/10.3390/s21196597

Li, Y., Chen, W., Yang, H., Li, J., & Zheng, N. (2020). Joint torque closed-loop estimation using NARX neural network based on sEMG signals. *IEEE Access*, *8*, 213636–213646. https://doi.org/10.1109/ACCESS.2020.3039983

Lim, H., Kim, B., & Park, S. (2019). Prediction of lower limb kinetics and kinematics during walking by a single IMU on the lower back using machine learning. *Sensors*, *20*(1), Article 130. https://doi.org/10.3390/s20010130

Liu, X., Zhou, Z., Mai, J., & Wang, Q. (2019). Real-time mode recognition based assistive torque control of bionic knee exoskeleton for sit-to-stand and stand-to-sit transitions. *Robotics and Autonomous Systems*, *119*, 209–220. https://doi.org/10.1016/j.robot.2019.06.008

Liu, Y., Shih, S. M., Tian, S. L., Zhong, Y. J., & Li, L. (2009). Lower extremity joint torque predicted by using artificial neural network during vertical jump. *Journal of Biomechanics*, *42*(7), 906–911. https://doi.org/10.1016/j.jbiomech.2009.01.033

McCabe, M. V., Citters, D. W. V., & Chapman, R. M. (2023). Hip joint angles and moments during stair ascent using neural networks and wearable sensors. *Bioengineering*, *10*(7), Article 784. https://doi.org/10.3390/bioengineering10070784

Molinaro, D. D., Kang, I., Camargo, J., & Young, A. J. (2020, November 29-December 1). *Biological hip torque estimation using a robotic hip exoskeleton*. [Paper presentation]. 8th IEEE RAS/EMBS International

Conference for Biomedical Robotics and Biomechatronics (BioRob), New York, USA. https://doi.org/10.1109/biorob49111.2020.9224334

Moreira, L., Figueiredo, J., Vilas-Boas, J. P., & Santos, C. P. (2021). Kinematics, Speed, and anthropometry-based ankle joint torque estimation: A deep learning regression approach. *Machines*, *9*(8), Article 154. https://doi.org/10.3390/machines9080154

Mundt, M., Johnson, W. R., Potthast, W., Markert, B., Mian, A., & Alderson, J. (2021). A comparison of three neural network approaches for estimating joint angles and moments from inertial measurement units. *Sensors*, *21*(13), Article 4535. https://doi.org/10.3390/s21134535

Mundt, M., Koeppe, A., David, S., Witter, T., Bamer, F., Potthast, W., & Markert, B. (2020). Estimation of gait mechanics based on simulated and measured IMU data using an artificial neural network. *Frontiers in Bioengineering and Biotechnology*, *8*, Article 41. https://doi.org/10.3389/fbioe.2020.00041

Naidu, G., Zuva, T., & Sibanda, E. M. (2023). A review of evaluation metrics in machine learning algorithms. In R. Silhavy & P. Silhavy (Eds.), *Artificial Intelligence Application in Networks and Systems* (pp. 15–25). Springer International Publishing. https://doi.org/10.1007/978-3-031-35314-7_2

Ozates, M. E., Karabulut, D., Salami, F., Wolf, S. I., & Arslan, Y. Z. (2023). Machine learning-based prediction of joint moments based on kinematics in patients with cerebral palsy. *Journal of Biomechanics*, *155*, Article 111668. https://doi.org/10.1016/j.jbiomech.2023.111668

Peng, L., Hou, Z. G., & Wang, W. (2015, August 25-29). *A dynamic EMG-torque model of elbow based on neural networks*. [Paper presentation]. 37th Annual International Conference of the IEEE Engineering in Medicine and Biology Society (EMBC*)*, Milan, Italy. https://doi.org/10.1109/EMBC.2015.7318986

Perera, C. K., Gopalai, A. A., Gouwanda, D., Ahmad, S. A., & Salim, M. S. B. (2023). Sit-to-walk strategy classification in healthy adults using hip and knee joint angles at gait initiation. *Scientific Reports*, *13*(1), Article 16640. https://doi.org/10.1038/s41598-023-43148-0

Pizzolato, C., Lloyd, D. G., Sartori, M., Ceseracciu, E., Besier, T. F., Fregly, B. J., & Reggiani, M. (2015). CEINMS: A toolbox to investigate the influence of different neural control solutions on the prediction of muscle excitation and joint moments during dynamic motor tasks. *Journal of Biomechanics*, *48*(14), 3929–3936. https://doi.org/10.1016/j.jbiomech.2015.09.021

Schmidt, K., Duarte, J. E., Grimmer, M., Sancho-Puchades, A., Wei, H., Easthope, C. S., & Riener, R. (2017). The myosuit: Bi-articular anti-gravity exosuit that reduces hip extensor activity in sitting transfers. *Frontiers in Neurorobotics*, *11,* Article 57. https://doi.org/10.3389/fnbot.2017.00057

Schulte, R. V., Zondag, M., Buurke, J. H., & Prinsen, E. C. (2022). Multi-day EMG-based knee joint torque estimation using hybrid neuromusculoskeletal modelling and convolutional neural networks. *Frontiers in Robotics and AI*, *9,* Article 869476. https://doi.org/10.3389/frobt.2022.869476

Seth, A., Hicks, J. L., Uchida, T. K., Habib, A., Dembia, C. L., Dunne, J. J., Ong, C. F., DeMers, M. S., Rajagopal, A., Millard, M., Hamner, S. R., Arnold, E. M., Yong, J. R., Lakshmikanth, S. K., Sherman, M. A., Ku, J. P., & Delp, S. L. (2018). OpenSim: Simulating musculoskeletal dynamics and neuromuscular control to study human and animal movement. *PLOS Computational Biology*, *14*(7), Article e1006223. https://doi.org/10.1371/journal.pcbi.1006223

Siu, H. C., Sloboda, J., McKindles, R. J., & Stirling, L. A. (2021). A neural network estimation of ankle torques from electromyography and accelerometry. *IEEE Transactions on Neural Systems and Rehabilitation Engineering*, *29*, 1624–1633. https://doi.org/10.1109/TNSRE.2021.3104761

Su, C., Chen, S., Jiang, H., & Chen, Y. (2020). Ankle joint torque prediction based on surface electromyographic and angular velocity signals. *IEEE Access*, *8*, 217681–217687. https://doi.org/10.1109/ACCESS.2020.3040820

Taye, M. M. (2023). Theoretical understanding of convolutional neural network: Concepts, architectures, applications, future directions. *Computation*, *11*(3), Article 52. https://doi.org/10.3390/computation11030052

Truong, M. T. N., Ali, A. E. A., Owaki, D., & Hayashibe, M. (2023). EMG-Based estimation of lower limb joint angles and moments using long short-term memory network. *Sensors*, *23*(6), Article 3331. https://doi.org/10.3390/s23063331

Wang, L., & Buchanan, T. S. (2002). Prediction of joint moments using a neural network model of muscle activations from EMG signals. *IEEE Transactions on Neural Systems and Rehabilitation Engineering*, *10*(1), 30–37. https://doi.org/10.1109/TNSRE.2002.1021584

Wang, M., Chen, Z., Zhan, H., Zhang, J., Wu, X., Jiang, D., & Guo, Q. (2023). Lower limb joint torque prediction using long short-term memory network and gaussian process regression. *Sensors*, *23*(23), Article 9576. https://doi.org/10.3390/s23239576

Winter, D. A. (2009). *Biomechanics and Motor Control of Human Movement* (4th ed.). Wiley. https://doi.org/10.1002/9780470549148.ch5

Xia, K., Huang, J., & Wang, H. (2020). LSTM-CNN architecture for human activity recognition. *IEEE Access*, *8*, 56855–56866. https://doi.org/10.1109/ACCESS.2020.2982225

Yu, Y., Chen, C., Zhao, J., Sheng, X., & Zhu, X. (2022). Surface electromyography image-driven torque estimation of multi-dof wrist movements. *IEEE Transactions on Industrial Electronics*, *69*(1), 795–804. https://doi.org/10.1109/TIE.2021.3050367

Zhang, L., Soselia, D., Wang, R., & Gutierrez-Farewik, E. M. (2022). Lower-limb joint torque prediction using LSTM neural networks and transfer learning. *IEEE Transactions on Neural Systems and Rehabilitation Engineering, 30*, 600–609. https://doi.org/10.1109/TNSRE.2022.3156786

Zhang, L., Soselia, D., Wang, R., & Gutierrez-Farewik, E. M. (2023). Estimation of Joint Torque by EMG-Driven Neuromusculoskeletal Models and LSTM Networks. *IEEE Transactions on Neural Systems and Rehabilitation Engineering: A Publication of the IEEE Engineering in Medicine and Biology Society*, *31*, 3722–3731. https://doi.org/10.1109/TNSRE.2023.3315373

Zhang, Q., Fragnito, N., Bao, X., & Sharma, N. (2022). A deep learning method to predict ankle joint moment during walking at different speeds with ultrasound imaging: A framework for assistive devices control. *Wearable Technologies*, *3*, Article e20. https://doi.org/10.1017/wtc.2022.18